Performance analysis of Graphene Bilayer Transistors through tight-binding simulations

Gianluca Fiori and Giuseppe Iannaccone
Dipartimento Ingegneria dell'Informazione: Elettronica, Informatica e Telecomunicazioni
Università di Pisa
Pisa, Italy, IT-56122
URL: http://monteverdi.iet.unipi.it/ fiori
Telephone: +39 050 2217596
Fax: +39 050 2217522

***Abstract*—A simulation study of a tunable-gap bilayer graphene FET with independent gates is performed with a numerical solver based on the self-consistent solution of the Poisson and Schrödinger equations within the NEGF formalism. The applied vertical field manages to induce an energy gap, but its value is not large enough to suppress band-to-band tunneling and to obtain acceptable $I_{\rm on}/I_{\rm off}$ ratio for CMOS device operation.**

I. Introduction

Graphene, an atomic layer of carbon atoms arranged in a two-dimensional (2D) honeycomb lattice, is one of the few examples of 2D crystals. Since its first experimental demonstration [1] in 2004, this material has attracted a huge scientific interest, due to the intriguing properties of the two dimensional electron gas (2DEG), such as the linear dispersion relation typical of Dirac fermions, the very large measured mobility [1], [2] and the large coherence length. The hunt for new device architectures and new channel material for next generations of semiconductor technology [3] could find an interesting target in graphene. The mobility values reported in the literature for graphene FETs exhibit a large range of variability (from 10^2 to 10^4 $\mathrm{cm^2V^{-1}s^{-1}}$), depending on the material synthesis method and on device processing. Recent studies indicate that the intrinsic mobility contribution has been estimated to exceed 2×10^5 $\mathrm{cm^2V^{-1}s^{-1}}$ [4]. This indicates that a large room for improvement is available by finding innovative processing solutions allowing to use the giant intrinsic mobility of graphene.

The exploitation of wide flakes of graphene as channel material for FETs has been first demonstrated in [5] and in [6], showing very poor $I_{\rm on}/I_{\rm off}$ ratios (smaller than 10) and a limited capability for digital electronics applications. Being 2D graphene a semimetal with zero band gap, it is impossible to effectively turn "off" its conduction. An energy gap can however be induced by cutting 2D graphene in very narrow stripes [7], the so-called graphene nanoribbons, obtained by means of lithographic patterning (electron beam lithography [8] or scanning probe lithography [9], [10]) or through chemical reaction [11]. In this way, a high $I_{\rm on}/I_{\rm off}$ ratio has been obtained, for example in [12], with performance comparable to small diameter carbon nanotube devices. In spite of these intriguing demonstrations, state-of-the-art lithographic techniques are far beyond required atomic precision.

Another possibility to define an energy gap without the need of highly precise lithography, is represented by stacking graphene in multilayers, like in bilayer graphene. Recently, theoretical models [13], [14] and experiments [15], [16], [17] have indeed shown that bilayer graphene has an energy gap controllable by a vertical electric field. One could exploit this property to use bilayer graphene as a channel material for FETs, defining an energy gap only when really needed, i.e. when the FET must be in the off state. A simulation study on this subject has been first addressed by means of the effective mass approximation in [18] and then by means of the tight-binding approach in [19]. An analytical model has been instead proposed in [20].

In this work, we present a numerical approach able to describe the electrical behavior of Bilayer Graphene (BG) FET with independent gate operation, based on atomistic numerical simulations. In particular, we have extended our in-house device simulator *NanoTCAD ViDES* [21], based on the Non-Equilibrium Green's Function formalism (NEGF), with a tight-binding Hamiltonian on a p_z orbital basis set in the real space.

II. Physical Models and Numerical Approach

The Poisson equation in the three-dimensional domain reads

$$\nabla \left[\epsilon(\vec{r})\nabla\phi(\vec{r})\right] \;=\; -q\left[p(\vec{r}) - n(\vec{r}) + \rho_{fix}\right], \qquad (1)$$

where $\phi(\vec{r})$ is the electrostatic potential, q is the electron charge, $\epsilon(\vec{r})$ is the dielectric constant, and ρ_{fix} is the fixed charge. The electron and hole concentrations (n and p, respectively) are computed by solving the Schrödinger equation with open boundary conditions, by means of the NEGF formalism [22].

The Green's function can then be expressed as

$$G(E) = \left[EI - H - \Sigma_S - \Sigma_D\right]^{-1}, \qquad (2)$$

where E is the energy, I the identity matrix, H the Hamiltonian of the BG, and Σ_S and Σ_D are the self-energies of the source and drain, respectively. Transport is here assumed to be completely ballistic, i.e. no self-energies accounting for inelastic scattering are considered.

978-1-4244-3927-0/09/$25.00 ©2009 IEEE

Let us focus our attention on H. In particular, the considered bilayer graphene Hamiltonian is expressed by means of an atomistic (p_z orbitals) real space basis, and it is composed by the two single layer graphene Hamiltonians, coupled by the t_p=0.35 eV hopping parameters in correspondence of overlaying atoms along the z direction [14], i.e. the direction perpendicular to the plane of graphene: the elementary cell (Fig. 1) is repeated periodically along the x and y directions. In particular, Bloch periodic boundary conditions are imposed along the x direction with period equal to $\Delta = \sqrt{3}a_{cc}$, where $a_{cc} = 0.144$ nm is the carbon-carbon bonding distance. In this way, the k_x wave vector appears in the Hamiltonian. Semi-infinite contacts have been instead modeled along the y direction by means of self-energies.

As an example, let us consider the simple cell shown in Fig. 1, composed by 12 atoms, 6 in the bottom layer and 6 in the upper layer, and ordered as shown in the picture (u and d are for upper and bottom layer, respectively). If t is the hopping parameter, H is a tridiagonal block matrix, whose elements are 2×2 matrices.

In particular, H reads

$$H = \begin{pmatrix} D_1 & \alpha & & & & \\ \alpha & D_2 & \beta_1 & & & \\ & \beta_1^\dagger & D_3 & \alpha & & \\ & & \alpha & D_4 & \beta_2 & \\ & & & \beta_2^\dagger & D_5 & \alpha \\ & & & & \alpha & D_6 \end{pmatrix}, \quad (3)$$

where

$$D_i = \begin{pmatrix} \Phi_{iu} & 0 \\ 0 & \Phi_{ib} \end{pmatrix}, \quad (4)$$

and Φ_{iu} and is Φ_{ib} are the potentials of the i-th couple of atoms, laying on the upper and on the bottom layer, respectively.

If we now define $\tilde{t}$ as

$$\tilde{t} = te^{ik_x\Delta}, \quad (5)$$

where i is the imaginary number, the off-diagonal block matrices read:

$$\alpha = \begin{pmatrix} t & 0 \\ 0 & t \end{pmatrix}, \quad (6)$$

$$\beta_1 = \begin{pmatrix} t+\tilde{t} & 0 \\ t_p & t+\tilde{t}^\dagger \end{pmatrix}, \quad (7)$$

and

$$\beta_2 = \begin{pmatrix} t+\tilde{t}^\dagger & 0 \\ t_p & t+\tilde{t} \end{pmatrix}. \quad (8)$$

A point charge approximation is assumed, i.e. all the free charge around each carbon atoms is spread with a uniform concentration in the elementary cell including the atom. Assuming that the electro-chemical potential of the reservoirs are aligned at the equilibrium with the Fermi level of the BG,

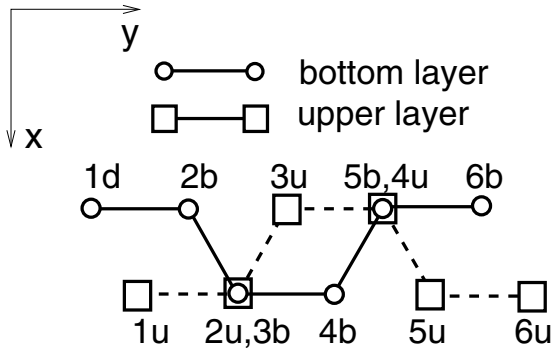

Fig. 1. Elementary cell of the simulated bilayer graphene

and given that there are no fully confined states, the electron concentration is

$$\begin{aligned} p(\vec{r}) - n(\vec{r}) &= 1 + 2\int_{BZ} dk_x \int_{-\infty}^{+\infty} dE \cdot \\ &\left[|\psi_{\mathrm{S}}(\mathrm{E}, \mathrm{k_x}, \vec{\mathrm{r}})|^2 f(E - E_{F_S}) \right. \\ &\left. + |\psi_{\mathrm{D}}(\mathrm{E}, \mathrm{k_x}, \vec{\mathrm{r}})|^2 f(E - E_{F_D})\right], \quad (9) \end{aligned}$$

where $\vec{r}$ is the coordinate of the carbon site, f is the Fermi-Dirac occupation factor, $|\psi_S|^2$ ($|\psi_D|^2$) is the probability that states injected by the source (drain) reach the carbon site $\vec{r}$, E_{F_S} (E_{F_D}) is the Fermi level of the source (drain), and the +1 term accounts for C atom ioniziation. The k_x integral is performed over the Brillouin zone (BZ).

The current has been instead computed as

$$\begin{aligned} I &= \frac{2q}{h}\int_{BZ} dk_x \int_{-\infty}^{+\infty} dE \cdot \\ &\mathcal{T}(E, k_x)\left[f(E - E_{F_S}) - f(E - E_{F_D})\right], \quad (10) \end{aligned}$$

where h is Planck's constant and $\mathcal{T}(E)$ is the transmission coefficient.

From a numerical point of view, when solving the integrals along the k_x axis, we have verified that 32 k values are enough in order to obtain accurate results. For what concerns instead the computation of the self-energy Σ, we have adopted the transfer Hamiltonian formalism as proposed by Sancho et al. [23], which works better than simple underelaxation techniques, in correspondence of the Van Hooven singularities: for each energy point, Σ is found with almost the same number of iterations (about 15). Transport computation can be still too computationally demanding, so that integration over the k axis has been parallelized by means of MPI subroutines.

The non-linear system has been solved with the Newton/Raphson (NR) method with the Gummel iterative scheme. In particular, the Schrödinger equation is solved at the beginning of each NR cycle of the Poisson equation, and the charge density in the BG is kept constant until the NR cycle converges (i.e. the correction on the potential is smaller than a predetermined value). The algorithm is then repeated cyclically until the norm of the difference between the potential computed at the end of two subsequent NR cycles is smaller than a predetermined value.

III. Results and Discussion

In Fig. 2 the energy dispersions for graphene bilayer BG are shown in correspondence of the Dirac point, for different values of V, i.e. the difference between the potential on the upper and the bottom layer. Due to the symmetry of the energy dispersion, the plot is shown only for $k_y = 0$.

As can be seen, for V=0 eV the BG has no energy gap, while a gap is induced for increasing values of V: the higher V, the higher the energy gap. In addition, the top and the bottom of the second and third subband, respectively, show the so-call "mexican-hat" behavior, i.e. we observe a local maximum in correspondence of the Dirac points, while the minimum is shifted by $k_g(V)$, which reads [14]

$$k_g = \sqrt{\frac{V^2 + 2t_p^2}{V^2 + t_p^2}} \frac{V}{2v_F}, \tag{11}$$

where v_F is the Fermi velocity, $v_F = \frac{3a_{cc}t}{2}$.

The simulated device is a double-gate BG-FET, whose structure is shown in Fig. 3. We assume metal gates, and a 1.5 nm layer of SiO_2 as gate dielectric. We also assume an air gap of 0.5 nm between the dielectric interface and the position of carbon sites. The channel is 15 nm long, and the inter-layer distance is 0.35 nm. The source and drain extensions are 10 nm long, and are doped with an equivalent molar fraction of fully ionized donors $f_d = 5 \times 10^{-3}$.

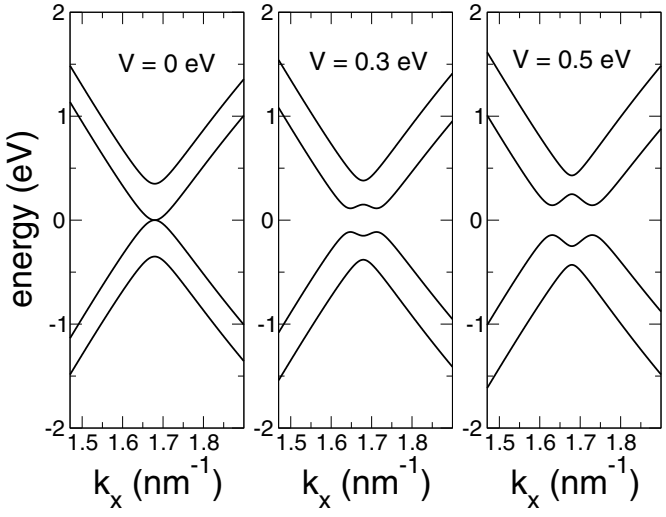

Fig. 2. Energy dispersion in correspondence of the Dirac point for different values of V, i.e. the difference between the potential on the top and on the botton layer.

In Fig. 4 the transfer characteristics for $V_{DS} = 0.5\ V$ are shown, for different gate configurations. In particular, in Fig. 4a the transfer characteristics as a function of the top gate voltage ($V_{\rm top}$) for different bottom gate voltages ($V_{\rm bottom}$) are shown. As can be seen, large currents can be obtained above threshold, while the BG-FET shows huge problems to switch off. Even after applying very negative gate voltages, the drain-to-source current decreases only by roughly a factor of six. The ratio even worsens when $V_{\rm bottom} = -1.0\ V$, since in this case

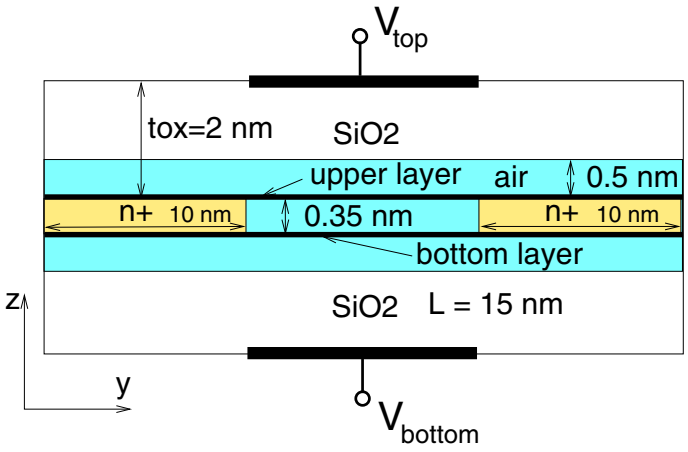

Fig. 3. Transversal cross-section of the simulated graphene bilayer field effect transistor.

a larger amount of positive charge is injected in the valence band, due to band-to-band tunneling, which pins the potential along the channel, and further degrades the gate control over the barrier.

In order to increase the vertical electric field between the two layers of graphene, we have driven the device by imposing a fixed voltage between the two gates $V_{\rm diff} = V_{\rm top} - V_{\rm bottom}$.

Even in this case, device transconductance (i.e. the slope of the transfer characteristic) almost remains the same, regardless of the applied $V_{\rm diff}$. This can be explained by the large accumulation of positive charge in the channel, caused by band-to-band tunneling in correspondence of the drain: this charge screens the vertical electric field, limiting the size of the opened bandgap.

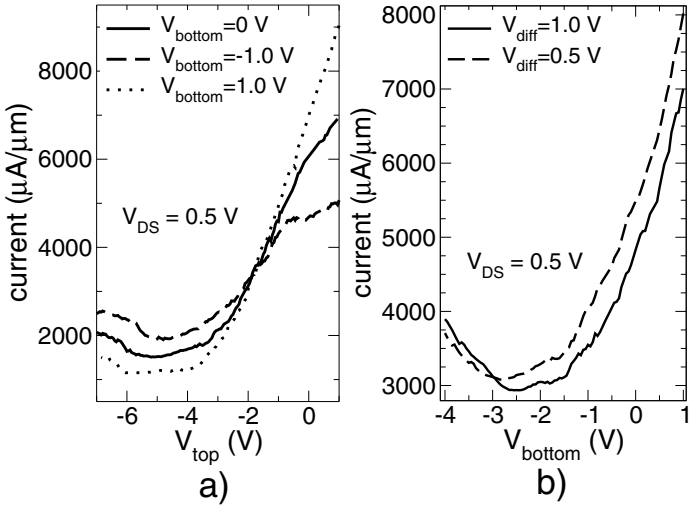

Fig. 4. a) Transfer characteristics computed as a function of the top gate voltage, when the bottom gate voltage $V_{\rm bottom}$=1.0 V (dotted line), $V_{\rm bottom}$=0 V (solid line) and $V_{\rm bottom}$=-1.0 V (dashed line); b) transfer characteristics computed as a function of $V_{\rm bottom}$ for $V_{\rm diff}$=1.0 V (solid line) and $V_{\rm diff}$=0.5 V (dashed line).

In Fig. 5, the transmission coefficients are plotted as a function of the energy and for different bias points. In par-

ticular, all the plots refer to the $V_{bottom} = 0$ V case, while $V_{DS} = 0.5$ V, and V_{top} =-0.5, -2.0 and -4.0 V. Source and drain Fermi level are also depicted. For energies included in the $[E_{FD}, E_{FS}]$ interval, we can observe a large band-to-band tunneling component, which degrades the transistor off-state. As stated above, this is due to the presence of bound states in the valence band, which are also responsible for the pinning of the channel potential. As indeed can be noted, despite the large applied V_{top} voltage (V_{top}=-4.0 V), the transmission coefficient is only slightly shifted as compared to the $V_{top} = -0.5$ V case.

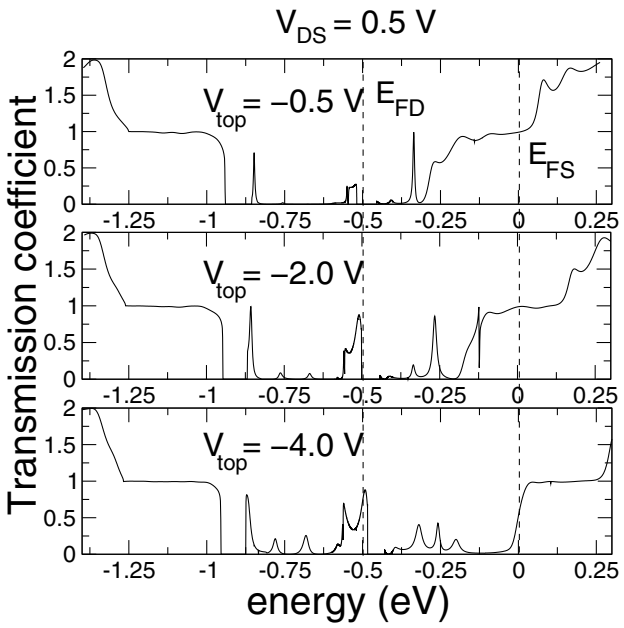

Fig. 5. Transmission coefficient in correspondence of the Dirac point, for $V_{DS} = 0.5$ V and different V_{top}.

IV. Conclusion

We have explored the possibility of realizing FETs by exploiting the tunable-gap property of bilayer graphene, through a code based on Tight-Binding NEGF device simulations. Aiming at technology foresight, we have considered the overly optimistic case of an ideal structure and of ballistic transport.

Our computer simulations show that tuning the gap is not a very promising technique for achieving appropriate switching characteristics of BG-FETs, due to the too weak suppression of band-to-band tunneling.

Acknowledgment

The work was supported in part by the EC Seventh Framework Program under project GRAND (Contract 215752), by the Network of Excellence NANOSIL (Contract 216171), and by the European Science Foundation EUROCORES Program Fundamentals of Nanoelectronics, through funds from CNR and the EC Sixth Framework Program, under project DEWINT (ContractERAS-CT-2003-980409). Authors gratefully acknowledge Network for Computational Nanotechnology (NCN) for providing computational resources through which part of the results here shown has been obtained.

References

[1] K. S. Novoselov, A. K. Geim, S. V. Morozov, D. Jiang, Y. Zhang, S. V. Dubonos, I. V. Grigorieva, and A. A. Firsov, Science, Vol. 306, No. 5696, p. 666 2004.
[2] C. Berger, Z. Song, X. Li, X. Wu, N. Brown, C. Naud, D. Mayou, T. Li, J. Hass, A. N. Marchenkov, E. H. Conrad, P. N. First, W. A. de Heer, Science, Vol. 312, p. 1191, 2006.
[3] International Technology Roadmap for Semiconductors 2007, Semiconductor Industry Association, S. Jose, USA, (http://public.itrs.net).
[4] J.H. Chen, C. Jang, S. Xiao, M. Ishigami, M. S. Fuhrer, Nature Nanotechnology, Vol. 3, p. 206, 2008.
[5] M. C. Lemme, T. J. Echtermeyer, M. Baus, and H. Kurz, IEEE Electr. Dev. Lett., Vol. 28, No. 4, p. 282, 2007.
[6] Z.Chen, Y-M. Lin, M. J. Rooks and P. Avouris, Physica E, Volume 40, p. 228, 2007.
[7] Y-W Son, M.L. Cohen, S.G. Louie, Phys. Rev. Lett. Vol. 97, p. 216803, 2006.
[8] M. Y. Han, B. Ozyilmaz, Y. Zhang, and P. Kim, Phys Rev Lett. Vol. 98, p. 206805, 2007.
[9] L. Tapaszto, G. Dobrik, P. Lambin, and L. P. Biro, Nature Nanotechnology, 3, 397 (2008).
[10] L. Weng, L. Zhang, Yong P. Chen, and L. P. Rokhinson, Appl. Phys. Lett 93, 093107 (2008).
[11] X. Li, X. Wang, L. Zhang, S. Lee, H. Dai, Science, Vol. 319, pp. 1229-1232, 2008.
[12] X. Wang, Y. Ouyang, X. Li, H. Wang, J. Guo, H. Dai, Phys Rev Lett, Vol. 100, p. 206803, 2008.
[13] E. McCann, V.I. Falko, Phys. Rev. Lett., Vol. 96, p. 086805, 2006.
[14] J. Nilsson, A.H. Castro Neto, F. Guinea, N.M.R. Peres, Phys. Rev. Lett., Vol. 97, p. 266801, 2006.
[15] E.V. Castro, K.S. Novoselov, S.V. Morozov, N.M.R. Peres, J.M.B Lopes dos Santos, J. Nilsson, F. Guinea, A.K. Geim, A.H. Castro Neto, Phys. Rev. Lett., Vol. 99, p. 216802, 2007.
[16] T. Ohta, A. Bostwick, T. Seyller, K. Horn, E. Rotenberg, Science, Vol. 313, pp. 951-954, 2006.
[17] J.B. Oostinga, H.B. Heersche, X. Liu, A.F. Morpurgo, Nature Material, Vol. 7, pp.151-157, 2008.
[18] Y. Ouyang, P. Campbell, J. Guo, Appl. Phys. Lett., Vol. 92, p. 063120, 2008.
[19] G. Fiori, G. Iannaccone, IEEE Electr. Dev. Lett., Vol.30, p.261, 2009.
[20] M.Cheli, G.Fiori, G.Iannaccone, available online at http://arxiv.org/abs/0812.4739
[21] See the website for the source code and the documentation. [Online]. Available: http://www.nanohub.org/tools/vides.
[22] S. Datta. *Superlattice and Microstructures*, Vol. 28, pp. 253-277, Jul. 2000.
[23] M. P. Lopez Sancho, J. M. Lopez Sancho, and J. Rubio, *J. Phys. F.*, Vol. 15, pp. 851-858, Oct. 1984.